J Mater Sci (2010) 45:582–588
DOI 10.1007/s10853-009-3930-9

Surface patterning nanoparticle-based arrays

Kathy Lu · Chase Hammond · Junmin Qian

Received: 19 June 2009 / Accepted: 24 September 2009 / Published online: 14 October 2009

Abstract In this study, focused ion beam lithography is used to pattern different size and shape island arrays on silicon wafers. Cavity arrays of inverse shapes are then made on silicone mold surfaces by polymerization. After that, Al_2O_3 nanoparticle-based island arrays are created by a surface feature transfer and freeze casting process using an Al_2O_3 colloidal suspension. The effects of silicone mold surface wettability and freezing rate on the Al_2O_3 nanoparticle pattern quality are investigated. The results show that coating the silicone mold surface with a 10 nm thick Au–Pt layer makes the Al_2O_3 nanoparticle suspension more wetting on the mold surface and also likely reduces the dry Al_2O_3 nanoparticle adhesion to the mold surface. Freezing rate should be lower than 1 °C/min to avoid cracks or loose Al_2O_3 nanoparticle packing in the freeze cast features. When these factors are properly controlled, the reported patterning process allows reproduction of micron-size feature arrays from Al_2O_3 nanoparticle suspensions. The studied approach should be applicable to most nanoparticle-based materials and open numerous opportunities for direct-device fabrication.

Introduction

Patterning has attracted considerable attention because of its potential applications in microelectronics [1, 2], optoelectronics, sensing [3], and biomedical devices [4]. The methods used for patterning can be classified into two categories: top–down and bottom–up. The top–down approach uses a patterned template as a mask/mold to create patterns. The process includes imprinting and lithographic patterning [5–7]. The top–down method has the advantages of precise control of feature size, easy preparation of patterns on masks/molds, and ability to fabricate large area patterns [8]. The bottom–up approach involves self-assembly of ions/molecules/nanoparticles on substrates via electrostatic attraction [9], van der Waals force, covalent bond [10], or molecular recognition [11]; it is usually used to obtain parallel or single-line patterns for device applications.

The top–down methods are preferred for creation of ordered patterns. The bottom–up methods can offer finer resolution but the process is time-consuming [12]. If the top–down and the bottom–up approaches can be combined, new pattern creation capability might be possible. For example, the combination of contact charge transfer and polydimethylsiloxane mold enabled deposition of patterned nanoparticles [12]. Chemically directed nanoparticle assembly in combination with nanoimprinting allowed patterning of nanoparticles on different substrates [13].

Nanoparticles are widely available and have been the subject of intensive research for many years because of their promising applications [14–16], such as photonics, electronics, catalysis [17], and sensing [18]. Nanoparticles can be used as simple and versatile building blocks to form new devices and three-dimensional structures when they are properly arranged and the inter-particle or particle/substrate interactions are properly invoked [19, 20].

One exciting area to explore is to use templated molds to regulate and confine nanoparticles into a pre-determined pattern arrays. The combination of templating and nanoparticle processing provides a simple and effective technique to pattern different types of nanoparticles and can be used for fabrication of novel micro- and even nano-devices

K. Lu (✉) · C. Hammond · J. Qian
Department of Materials Science and Engineering, Virginia Polytechnic Institute and State University, 213 Holden Hall-M/C 0237, Blacksburg, VA 24061, USA
e-mail: klu@vt.edu

[21]. The process consists of three consecutive transfer steps: patterning of mold core, mold making, and nanoparticle-based feature creation [22]. However, formation of patterns with good feature fidelity and integrity is still a challenge. The interaction between a specific nanoparticle suspension and the corresponding mold surface needs to be better understood in order to avoid feature sticking and breakage. Also, packing of deposited nanoparticles needs to be reasonably dense in order to retain the formed feature arrays.

In this work, a nanoparticle-based surface templating process is studied. First, silicone molds are made by focused ion beam (FIB) lithography and templated feature array transfer. Second, a 35 vol% solids loading Al_2O_3 nanoparticle suspension is produced. Finally, different Al_2O_3 nanoparticle-based feature arrays are obtained by freeze casting. Wettability of the Al_2O_3 nanoparticle suspension on the silicone mold surface and freezing rate are studied in order to obtain well-defined feature arrays. This templating and freeze casting approach allows creation of micron-size feature arrays from the Al_2O_3 nanoparticle suspension.

Experimental procedure

Mold making

In this study, Si wafer (p type, (100) orientation) was used as the mold core and was first patterned using a dual beam FIB microscope (FEI Helios 600 NanoLab, Hillsboro, OR). The instrument was composed of a sub-nanometer resolution field emission scanning electron microscope (SEM) and a field emission scanning Ga^+ beam column. Samples can be moved by 150 mm distance along *X* and *Y* axes and tilted from $-5°$ to 60° by a high precision specimen goniometer. The Ga^+ source had a continuously adjustable energy range from 0.5 to 30 kV and an ion current between 1.5 pA and 21 nA. The patterning beam spot size and resolution were a function of the ion beam current and voltage and can be tuned to as small as 5 nm. The FIB microscope can read 24 bit digital patterns and reproduce them on a substrate using the ion beam.

Silicone molds were produced using the templated silicon wafer as the mold core [23–27]. First, the patterned silicon wafer was glued onto a 25 mm diameter and 2.5 mm thick aluminum disk. Silicone base compounds and curing agent (RTV 664, General Electric Company, Waterford, NY) were homogeneously mixed at 10:1 ratio before being poured over the silicon wafer and the aluminum disk assembly. A 30 mm diameter and 10 mm high plastic tube with a 1.0 mm thick wall was used to obtain a short silicone cylinder. The silicon wafer/aluminum disk assembly and the silicone mixture were placed under 40 Pa pressure for the removal of the air bubbles in the silicone compounds. Since the silicone mixture had high viscosity, the vacuuming process was repeated three to five times before being kept at 40 Pa for 15 minutes. Then the silicone mixture was cured for 24 hrs at ambient conditions before being separated from the silicon wafer. One end of the silicone cylinder receded inwards with a 1.5 mm thick wall and the receded surface was defined by the assembled aluminum disk and the silicon wafer. The silicone sample was termed 'mold' in this study.

Al_2O_3 suspension preparation

Al_2O_3 nanoparticles with a specific surface area of 45 m^2/g were used in this study (Nanophase Technologies, Romeoville, IL). Average Al_2O_3 particle size was around 38 nm with a normal size distribution from 10 to 50 nm [23]. For the Al_2O_3 nanoparticle suspension preparation, poly(acrylic acid) (PAA, M_W 1,800, Aldrich, St Louis, MO) was used as a dispersant; glycerol ($C_3H_8O_3$, Fisher Chemicals, Fairlawn, NJ) was used as an anti-freezing agent. A water-glycerol mixture at a ratio of 9:1 (water:glycerol) was used as the dispersing medium. The mixture was homogenized for 5 min using a ball mill before use. Al_2O_3 nanoparticles were added into the dispersing medium in 10 g increments along with 2.0 wt% of PAA dispersant (on Al_2O_3 basis). Since low pH promotes PAA dispersant adsorption onto Al_2O_3 nanoparticles [28], HCl solution was added to lower the pH to 1.5. The suspension was ball milled for 12 hrs with periodic adjustment of pH to 1.5. Suspensions of approximately 20 vol% Al_2O_3 solids loading were made by this procedure. After this step, Al_2O_3 nanoparticles were again added in 10 g increments, along with 2.0 wt% of PAA dispersant (on Al_2O_3 basis) to make 35 vol% solids loading suspension. NH_4OH was used to adjust the suspension pH to 9.5. The suspension was then mixed for 24 hrs for complete homogenization.

Contact angle measurement

The contact angle between the Al_2O_3 nanoparticle suspension and the silicone mold was measured using a 3D Digital Video Microscope (KH-7700, Hirox-USA, Inc., River Edge, NJ). First, the Al_2O_3 nanoparticle suspension was placed on the surface of the silicone mold by a syringe (1 cc 25G 5/8 Tuberculin, Becton–Dickinson & Company, Franklin Lakes, NJ). Then the droplet and the silicone mold images were taken using the microscope. The contact angle was measured from the images. An average value from ten different measurements was taken as the final contact angle result.

Table 1 The experimental parameters varied in this study

Mold surface coating	Freezing rate (°C/min)
With Au–Pt coating	1.0
	0.5
	0.25
	0.05
Without Au–Pt coating	1.0
	0.5
	0.25
	0.05

Templated feature array making and characterization

For one set of the silicone molds, a 10 nm Au–Pt layer was applied onto the mold surface by a physical sputtering process. The Al_2O_3 nanoparticle suspension was filled into the two sets of the silicone molds (with and without the Au–Pt layer) immediately after the suspension preparation using a disposable pipette. Care was taken to completely fill the molds and avoid air bubbles. The filled molds were kept under ambient conditions for 1 hr. After this pre-rest, the samples were frozen in a freeze dryer (AdVantage El-53, SP Industries Inc., Warminster, PA). The freezing rate was varied from 0.05 to 1 °C/min. The freezing temperature was −35 °C. The samples were kept at −35 °C for 2 hrs before the chamber pressure was decreased to 1 Pa. The filled molds were kept at −35 °C and 1 Pa pressure for 10 hrs before returning to room temperature in stages (−20 °C for 8 h, −10 °C for 4 h, −5 °C for 5 h, and 5 °C for 5 h). During the entire process, a pressure of 1 Pa was maintained. The experimental parameters varied in this study are given in Table 1.

The templated patterns and microstructural differences of the freeze cast features were analyzed using a LEO550 field emission SEM (Carl Zeiss MicroImaging, Inc, Thornwood, NY). To illustrate the three-dimensional nature of the templated features, the SEM images of the patterned arrays were taken at 45° tilt angle.

Results

Template and mold making

As pointed out, two steps are used in making the freeze casting molds. The first step is patterning the silicon mold core with the designed patterns. The second step is making the silicone molds using the patterned mold core. For the silicon mold core templating, the FIB voltage is 30 kV and the beam current is 21 nA. The patterns produced by the FIB lithography are shown in Fig. 1. There are three different patterns: homogenous circle array, heterogeneous circle array, and homogenous square array. Each array size is 100 × 100 μm. The larger size circles are 10 μm in diameter, the small size circles are 5 μm in diameter, and the squares are 10 μm in edge length. The feature-to-feature distance is 15 μm.

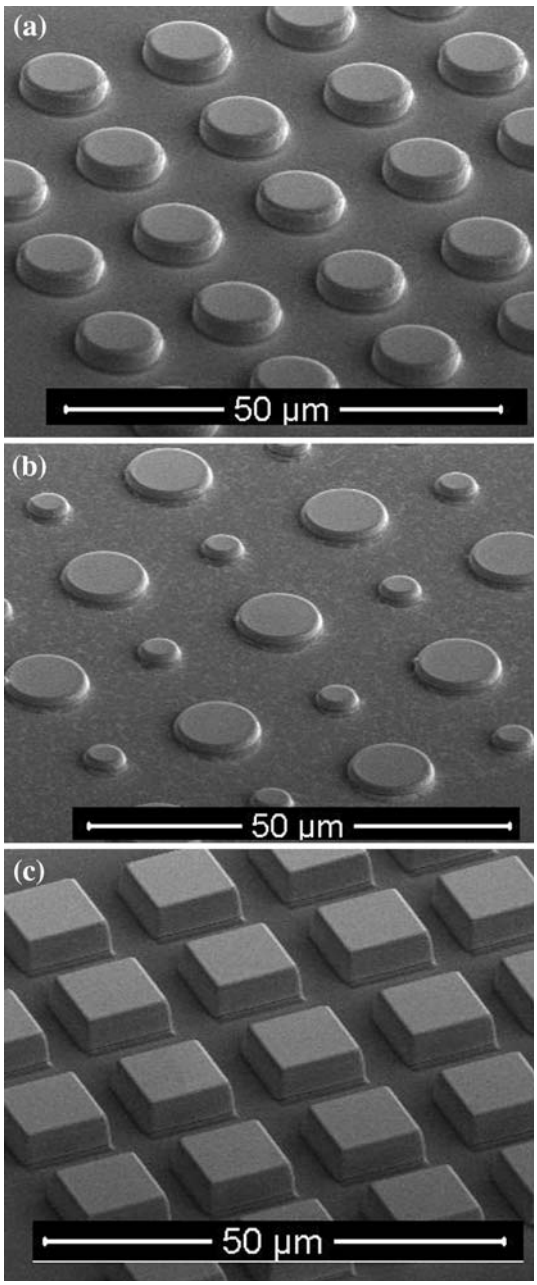

Fig. 1 SEM images of feature arrays produced by FIB lithography: **a** homogeneous circle array, **b** heterogeneous circle array, and **c** homogeneous square array

Under 30 kV voltage and 21 nA beam current patterning condition, the arrays generated have well-defined size, shape, and feature arrangement. The surfaces of different features are smooth. The feature height is controlled by the

patterning time and can be easily varied. The height of the homogenous circle and square island arrays is 4.8–5.0 μm. The height of the heterogeneous circle array is ~2.5 μm. During the FIB patterning, it is important to obtain well-focused ion beam. Good beam focus produces smoother feature surfaces in a faster rate [29]. However, it should be pointed out that the patterned feature shapes in Fig. 1 are slightly tapered in the height direction. This is a result of the Gaussian distribution shape of the ion beam. The diameter of the ion beam increases as its upper portion interacts with the silicon feature side surface. Scanning of the ion beam removes materials from the sides of the features while the features grow taller.

Figure 2 shows the SEM images of the silicone molds with different feature arrays. The feature arrays are accurately produced from the silicon mold core in an inverse manner. The new cavity features are well-defined and free of porosity or shape distortion. The feature size and spacing stay the same as those of the templated silicon mold core. The depth of the heterogeneous round cavity features is roughly half of those of the homogeneous round and square cavity features (approximately 5.0 vs. 2.5 μm). The large flaw on one of the square features in Fig. 2c is the result of a chip-off on the silicon mold core, demonstrating the feature array's reproducibility. It should also be mentioned that silicone is a very affordable mold material and widely available. The mold making process can be done in a short time. These characteristics make silicone a very attractive mold material for large surface area patterning.

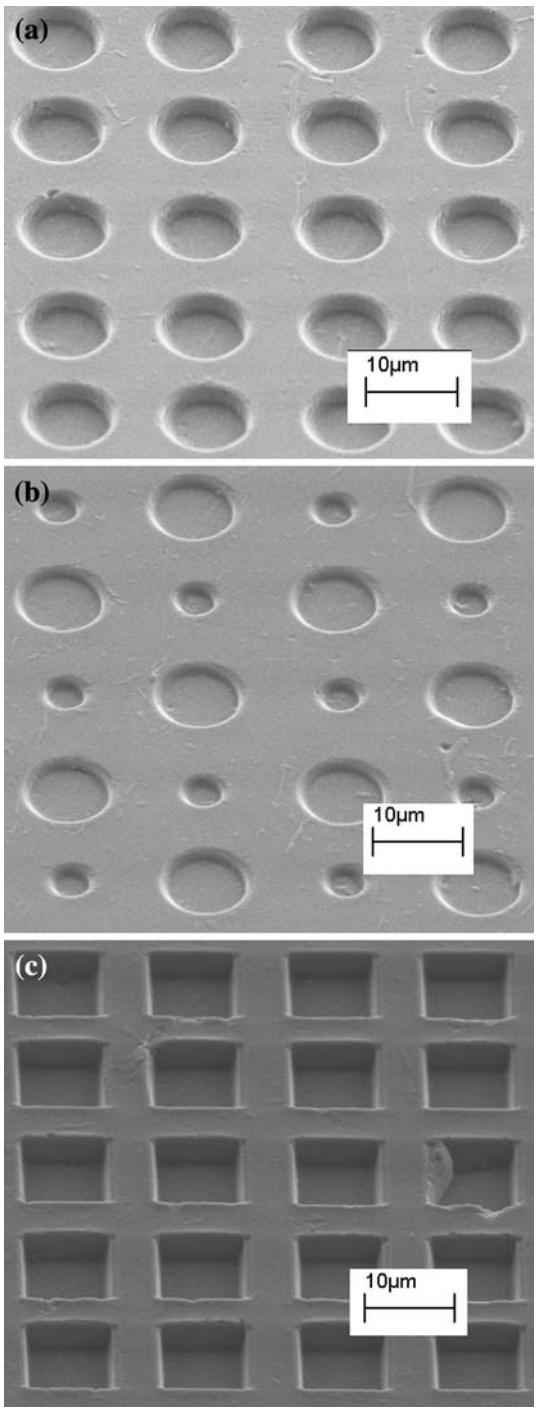

Fig. 2 SEM images of silicone mold cavity arrays: **a** homogeneous circle cavity array, **b** heterogeneous circle cavity array, and **c** homogeneous square cavity array

Templating

Formation of solid Al_2O_3 nanoparticle feature arrays is sensitive to the freeze casting conditions [22]. A pre-rest of an hour has to be used in accordance with previous work in order to effectively remove the air bubbles trapped inside the Al_2O_3 nanoparticle suspension [25, 26]. The island arrays produced from the silicone molds by the freeze casting process are shown in Fig. 3. The freezing rate used is 0.25 °C/min. The templated feature shapes are severely distorted. The Al_2O_3 nanoparticle suspension seems to adhere to the silicone mold surface during the freeze casting process. At the same time, the bonding between the Al_2O_3 nanoparticles is weak for all the freeze casting conditions. As a result, some of the templated Al_2O_3 features are stuck in the silicone mold cavities during the mold release. Apparently, the smaller circle features have the most severe shape distortion.

Au–Pt nanolayer effect

To address the distortion and breakage problem of the templated Al_2O_3 nanoparticle features, a 10-nm Au–Pt layer is applied onto the silicone mold surface as stated. With the surface coated molds, the designed feature arrays are reproduced with good fidelity under the same freezing casting conditions (Fig. 4). For the freeze cast Al_2O_3 nanoparticle feature arrays, there are almost no cracks or fractures on the features, most noticeably for the square

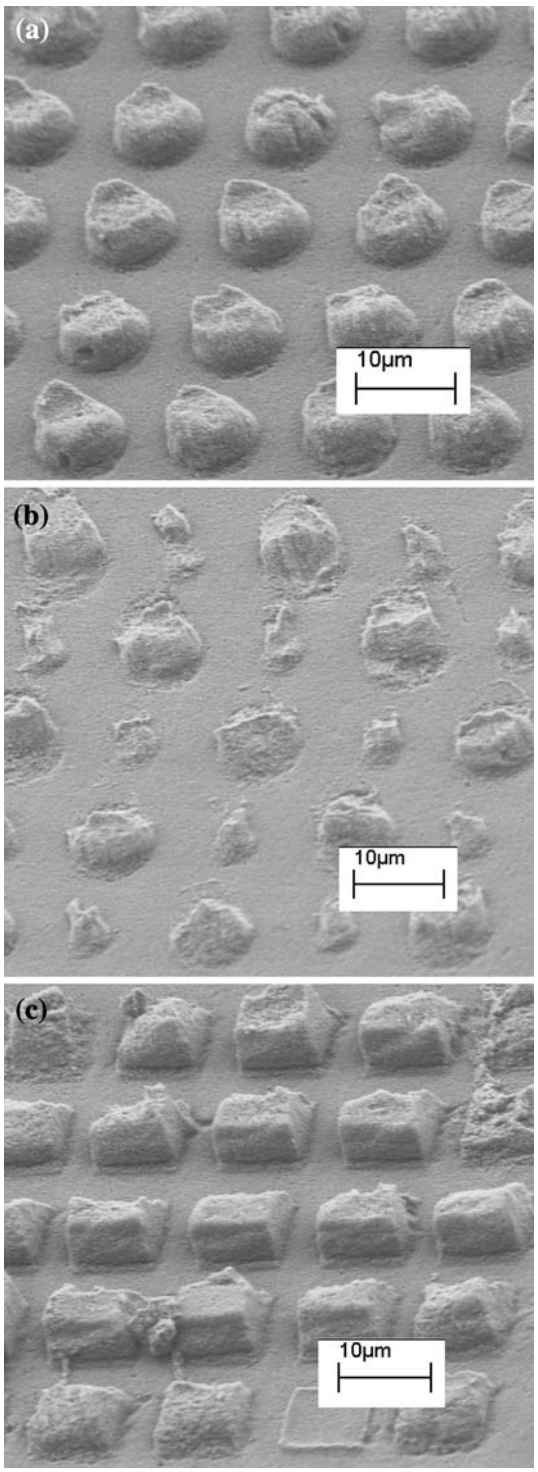

Fig. 3 Different Al_2O_3 nanoparticle feature arrays made from the silicone molds: **a** homogeneous circle array, **b** heterogeneous circle array, and **c** homogeneous square array

features. Again the defect due to the chip-off from the silicon wafer is reproduced. The debris on the templated array surfaces was created during handling. This means the silicone mold can maintain its rigidity and templated mold

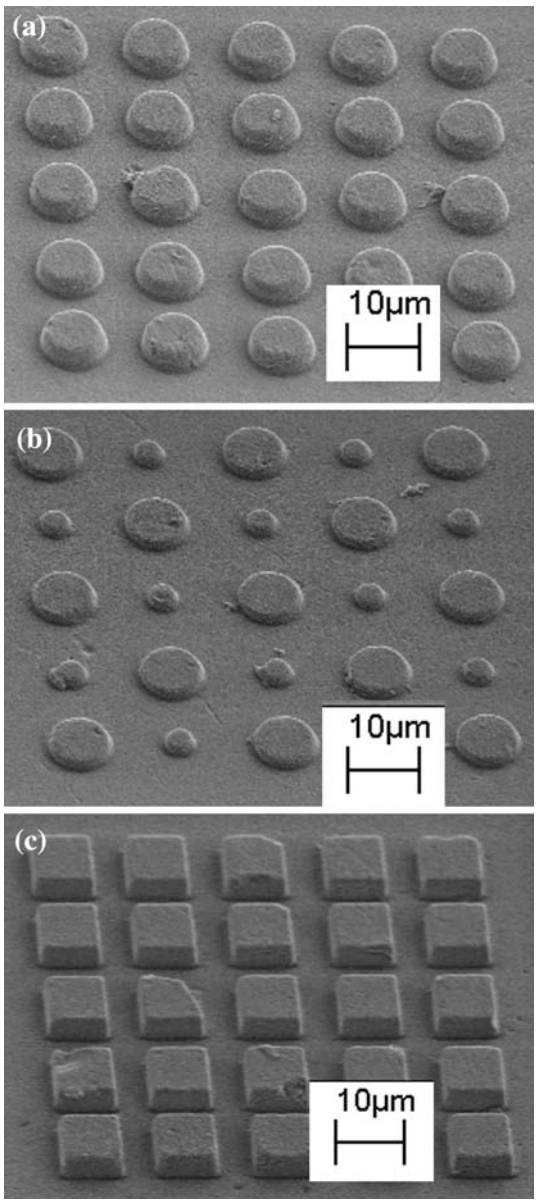

Fig. 4 Al_2O_3 nanoparticle patterns produced from the silicone mold coated with a 10 nm thick Au–Pt layer: **a** homogenous round island array, **b** heterogeneous round island array, and **c** homogenous square island array

shapes at the freeze casting condition. The poor feature reproducibility from the Al_2O_3 nanoparticle suspension most likely results from the incomplete suspension filling of the mold cavities and the mold surface sticking.

Coating the molds with a Au–Pt nanolayer shows to be an effective approach to reducing the patterned feature distortion and damage. The fundamental cause for the distortion of the features seen in Fig. 3 can be understood by examining the freeze casting process in two stages: the wet stage of the Al_2O_3 nanoparticle suspension and the dry stage of the Al_2O_3 nanoparticles in the molds.

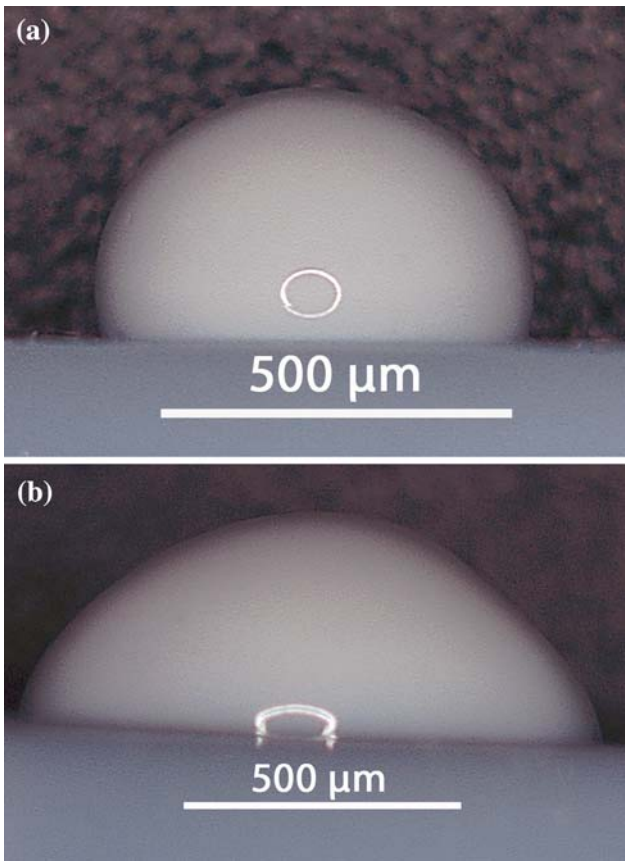

Fig. 5 Micrographs of Al_2O_3 nanoparticle suspension contact with the silicone mold: **a** no Au–Pt nanolayer, **b** with Au–Pt nanolayer

In the wet state, there is higher than desired interfacial energy, or affinity, between the silicone mold and the Al_2O_3 nanoparticle suspension. Figure 5 shows the optical micrographs of the Al_2O_3 nanoparticle suspension drops on the silicone mold surface without and with the Au–Pt nanolayer. As shown, the contact angle between the silicone surface and the Al_2O_3 nanoparticle suspension is 110° and 79.25°, respectively, without and with the Au–Pt nanolayer. This means that the Au–Pt nanolayer improves the surface wettability of the silicone molds by the Al_2O_3 nanoparticle suspension and thus the spreading of the Al_2O_3 nanoparticle suspension in the mold cavities. This can be explained as follows. Silicone is a polymeric material and hydrophobic. The Al_2O_3 nanoparticle suspension, on the other hand, is water-based and thus hydrophilic. The interfacial energy for the uncoated silicone mold-Al_2O_3 suspension contact is thus high because of the intrinsic difference in material behaviors. When the silicone mold is coated with the Au–Pt nanolayer, the surface becomes more hydrophilic and thus more wettable by the Al_2O_3 nanoparticle suspension. This reduces the interfacial energy and facilitates the spreading and filling of the Al_2O_3 nanoparticle suspension in the mold cavity arrays.

After the Al_2O_3 nanoparticle samples are dried, the removal process from the silicone molds is affected by the mold surface smoothness. With the Au–Pt coating, the mold surface should be smoother since the Au–Pt layer is only 10 nm thick. The Au–Pt nanolayer decreases the adhesion between the silicone mold and the Al_2O_3 nanoparticle sample. This facilitates the Al_2O_3 sample removal process without causing undesirable feature damage.

It should be pointed out that the above explanations need to be experimentally verified to be sure. Also, the Au–Pt nanolayer is very thin and should not be scratched in order to avoid damage. The Au–Pt nanolayer can stick to the Al_2O_3 nanoparticle sample and get removed from the mold surface during the mold release. So the Au–Pt nanolayer is mostly only effective for one time use.

Freezing rate effect

Freezing rate is the most significant parameter affecting the integrity of the freeze cast features. Figure 6 shows the freezing rate effect on the Al_2O_3 nanoparticle sample microstructures. The images are obtained from the as-cast surfaces. At 1 °C/min freezing rate (Fig. 6a), the nanoparticles have poor packing. Pores are common as a result of loose nanoparticle packing. At $\leq$0.5 °C/min freezing rates (Fig. 6b–d), Al_2O_3 nanoparticles show much denser packing and smoother surface. This means slower cooling rate is necessary for obtaining well-packed Al_2O_3 nanoparticle features. At a larger scale across the sample, the 1 °C/min freezing rate sample breaks easily. The $\leq$0.5 °C/min freezing rate samples have good integrity. Fast freezing rate results in an increase in the porosity of the templated Al_2O_3 nanoparticle samples and substantially lowers patterned feature integrity. Slower freezing rate can reduce the porosity and improve the integrity of the Al_2O_3 nanoparticle sample. The freezing rate for the 35 vol% solids loading Al_2O_3 suspension needs to be 0.5 °C/min or less. These results mean that the Al_2O_3 nanoparticle suspension requires time to rearrange and ice formation should be slow in order to maintain good Al_2O_3 nanoparticle arrangement.

Conclusions

Al_2O_3 nanoparticle-based feature arrays are patterned by a surface templating and freeze casting process. Mold surface wettability and freezing rate greatly affect the pattern quality and the feature microstructures. Coating the silicone mold surface with a 10-nm thick Au–Pt layer makes the surface more wetting for the Al_2O_3 nanoparticle suspension and also likely reduces the dry Al_2O_3 nanoparticle adhesion to the mold surface. Freezing rate should be lower than 1 °C/min in order to avoid microcracks and loose

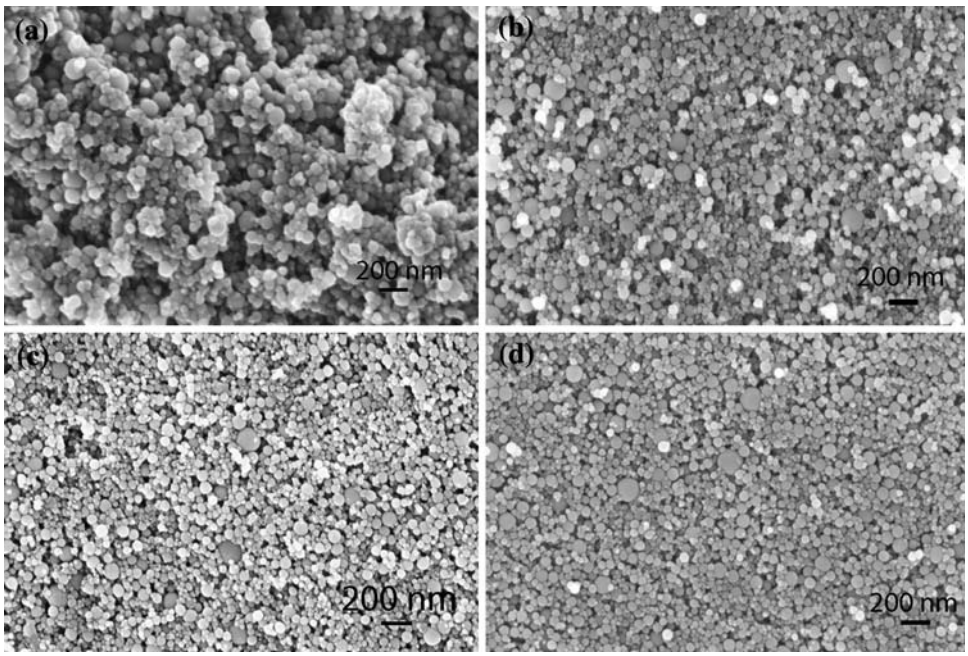

Fig. 6 SEM images of freeze cast Al_2O_3 microstructures at different freezing rates: **a** 1.0 °C/min, **b** 0.5 °C/min, **c** 0.25 °C/min, and **d** 0.05 °C/min

nanoparticle packing for the freeze cast features. When these factors are properly controlled, the patterning and freeze casting process allows reproduction of different micron-size feature arrays. This approach should be applicable to most nanoparticle suspensions and open numerous opportunities for direct-device fabrication.

Acknowledgement The authors acknowledge the financial support from National Science Foundation under Grant No. CMMI-0824741.

References

1. Shapley JDL, Barrow DA (2001) Thin Solid Films 388:134
2. Huang J, Moriyoshi T, Manabe H (2006) J Mater Sci 41:1605. doi:10.1007/s10853-006-4655-7
3. Huwiler C, Halter M, Rezwan K, Falconnet D, Textor M, Vörös J (2005) Nanotechnology 16:3045
4. Asoh H, Sakamoto S, Ono S (2007) J Colloid Interface Sci 316:547
5. Park I, Ko SH, Pan H, Grigoropoulos CP, Pisano AP, Fréchet JMJ, Lee ES, Jeong JJ (2008) Adv Mater 20:489
6. Liu K, Ho CL, Aouba S, Zhao YQ, Lu ZH, Petrov S, Coombs N, Dube P, Ruda HE, Wong WY, Manners I (2008) Angew Chem Int Ed 47:1255
7. Xia D, Li D, Luo Y, Brueck SRJ (2006) Adv Mater 18:930
8. Jung B, Frey W (2008) Nanotechnology 19:145303
9. Ofir Y, Samanta B, Xiao QJ, Jordan BJ, Xu H, Arumugam P, Arvizo R, Tuominen MT, Rotello VM (2008) Adv Mater 20:2561
10. Park JI, Lee WR, Bae SS, Kim YJ, Yoo KH, Cheon JW, Kim S (2005) J Phys Chem B 109:13119
11. Brom CRVD, Arfaoui I, Cren T, Hessen B, Palstra TTM, Hosson JTMD, Rudolf P (2007) Adv Funct Mater 17:2045
12. Kang M, Kim H, Han BW, Suh JS, Park JH, Choi MS (2004) Microelectronic Eng 71:229
13. Maury P, Escalante M, Reinhoudt DN, Huskens J (2005) Adv Mater 17:2718
14. Ma B, Ma J, Goh GKL (2008) J Mater Sci 43:4297. doi:10.1007/s10853-008-2627-9
15. Yoldi M, Gonzalez-Vinas W, Arcos MC, Sirera R (2006) J Mater Sci 41:2965. doi:10.1007/s10853-006-6717-2
16. Crocker M, Graham UM, Gonzalez R, Jacobs G, Morris E, Rubel AM, Andrews R (2007) J Mater Sci 42:3454. doi:10.1007/s10853-006-0829-6
17. Sreethawong T, Chavadej S, Ngamsinlapasathian S, Yoshikawa S (2008) Microporous Mesoporous Mater 109:84
18. Han L, Shi XJ, Wu W, Kirk FL, Luo J, Wang LY, Mott D, Cousineau L, Lim SI, Lu S, Zhong CJ (2005) Sens Actuators B 106:431
19. Puetz J, Aegerter MA (2008) Thin Solid Films 516:4495
20. Lin HY, Tsai LC, Chen CD (2007) Adv Funct Mater 17:3182
21. Cui TH, Hua F, Lvov Y (2004) Sens Actuators A 114:501
22. Lu K, Hammond C, Int J Appl Ceram Technol (submitted)
23. Lu K, Zhu X (2008) Int J Appl Ceram Technol 5(3):219
24. Lu K (2008) J Mater Sci 43(2):652. doi:10.1007/s10853-007-2155-z
25. Lu K (2007) J Am Ceram Soc 90(12):3753
26. Lu K, Kessler CS, Davis RM (2006) J Am Ceram Soc 89:2459
27. Lu K, Kessler CS (2006) In: Mullins WN, Wereszczak A, Lara-Curzio E (eds) Ceram engineering and science proceedings, vol 27(8), pp 1–10
28. Cesarano J, Aksay IA (1988) J Am Ceram Soc 71:1062
29. Lu K (2009) J Nanosci Nanotechnol 9:2598